CO2 capture from natural gas combined cycles by CO2 selective membranes

CO_2 capture from natural gas combined cycles by CO_2 selective membranes

Turi D.M.[a], Ho M.[b], Ferrari M.C[c], Chiesa P.[a], Wiley D.E.[b], Romano M.C.[a]

[a] Politecnico di Milano, Department of Energy, via Lambruschini 4, 20156 Milano, Italy

[b] The University of Sydney, School of Chemical and Biomolecular Engineering, NSW 2006, Sydney, Australia

[c] University of Edinburgh, School of Engineering, Robert Stevenson Road, Edinburgh EH9 3FB, United Kingdom.

Abstract

This paper performs a techno-economic analysis of natural gas-fired combined cycle (NGCC) power plants integrated with CO_2 selective membranes for post-combustion CO_2 capture. The configuration assessed is based on a two-membrane system: a CO_2 capture membrane that separates the CO_2 for final sequestration and a CO_2 recycle membrane that selectively recycles CO_2 to the gas turbine compressor inlet in order to increase the CO_2 concentration in the gas turbine flue gas. Three different membrane technologies with different permeability and selectivity have been investigated. The mass and energy balances are calculated by integrating a power plant model, a membrane model and a CO_2 purification unit model. An economic model is then used to estimate the cost of electricity and of CO_2 avoided. A sensitivity analysis on the main process parameters and economic assumptions is also performed. It was found that a combination of a high permeability membrane with moderate selectivity as a recycle membrane and a very high selectivity membrane with high permeability used for the capture membrane resulted in the lowest CO_2 avoided cost of 75 US\$/$t_{CO2.}$ This plant features a feed pressure of 1.5 bar and a permeate pressure of 0.2 bar for the capture membrane. This result suggests that membrane systems can be competitive for CO_2 capture from NGCC power plants when compared with MEA absorption. However, to achieve significant advantages with respect to benchmark MEA capture, better membrane permeability and lower costs are needed with respect to the state of the art technology. In addition, due to the selective recycle, the gas turbine operates with a working fluid highly enriched with CO_2. This requires redesigning gas turbine components, which may represent a major challenge for commercial deployment.

Keywords: CO_2 membranes, combined cycle, carbon capture, CCS, economic analysis

Nomenclature

CCA	Cost of CO_2 Avoided
CCM	Carbon Capture Membrane
CCS	Carbon Capture and Storage

COE	Cost of Electricity
CPU	Cryogenic Purification Unit
CRM	Carbon recirculation membrane
E	Specific CO_2 emissions [kg/MWh]
f	friction factor
e.m.	Electric motor
GT	Gas turbine
HRSG	Heat recovery steam generator
int	Interface
J	Flux through membrane [mol/s/m^2]
j	Flux through membrane [mol/s]
K	Permeance [gpu] or [mol/s/m^2/Pa]
LHV	Lower Heating Value
MEA	Monoethanolamine
MTR	Membrane Technology & Research
$\dot{n}$	Mole flow of a specific specie [mol/s]
NGCC	Natural gas combined cycle
perm	Permeate side of the membrane
PIM	Polymers of Intrinsic Microporosity
ref	Reference power plant without CO_2 capture
RH	Reheater
SH	Superheater
SPECCA	Specific primary energy consumption for CO_2 avoided [MJ_{LHV}/kg_{CO2}]
TIT	Turbine inlet temperature (total temperature at 1st rotor inlet)
TOT	Turbine outlet temperature
x	Mole fraction
Greek	
η_{pol}	Polytropic efficiency

1 Introduction

Membranes for CO_2 separation are receiving growing attention for application in the field of carbon capture and storage (CCS). Membrane separation is a continuous process that is attractive compared with absorption technologies for CCS because it does not require heat for regeneration and therefore does not affect steam turbine operations in the power plant. It can also be applied in energy intensive industries both as post-combustion and pre-combustion capture. In developing membrane processes for post-combustion carbon capture, the technical challenges arise due to the low partial pressure of CO_2 in the flue gas. Research efforts have been mostly focused on materials development in order to improve the permeability and selectivity with respect to the state-of-the-art materials. It is well known that performance of polymeric membranes, the most investigated CO_2 membrane technology, is characterized by an 'upper bound' that correlates permeability and selectivity (Robeson, 2008). In other words, polymeric membranes with high permeability usually have low selectivity and vice-versa, as explained theoretically by Freeman (Freeman, 1999). In addition to membrane materials, research has been conducted on the integration of the membrane separation process within the power plant.

The application as post-combustion capture systems in coal fired power plants has received the largest attention from researchers (Ho et al., 2008; Merkel et al., 2010; Scholes et al., 2013; Zhao et al., 2010) due to the higher partial pressure of CO_2 in the feed stream that facilitates the membrane separation. Different configurations with two or more membrane modules in series or parallel to achieve high CO_2 capture rate and high purity with the lowest cost have been examined.

Integration of CO_2 membranes in natural gas combined cycles (NGCCs) is more challenging, due to the much lower CO_2 content in the flue gases with respect to coal plants. Nevertheless, some studies have focused on using membranes for carbon capture in natural gas power plants (González-Salazar, 2015; Swisher and Bhown, 2014). In order to increase the CO_2 partial pressure in the membrane feed, Merkel et al. (Merkel et al., 2013) proposed a novel configuration with two membranes in series, where one membrane is used for a selective CO_2 recycle to the gas turbine (GT) compressor inlet, significantly increasing the CO_2 content in the flue gas and facilitating the CO_2 separation in the other membrane.

The aim of this paper is to assess the thermodynamic performance and economics of the integration of CO_2 membranes in NGCCs according to such a process configuration, performing sensitivity analyses on the main process variables and economic assumptions.

2 Methodology

2.1 Power plant model

The power plant integrated with CO_2 separation membranes assessed in this work follows the concept proposed in (Merkel et al., 2013) and is shown in Figure 1. The system is based on two membranes operating in series on the flue gas exiting the heat recovery steam generator (HRSG). The first one is the CO_2 capture membrane (CCM), which is a 3-port module (i.e. with no sweep gas on the permeate side), using a vacuum pump to keep a sub-atmospheric pressure on the permeate stream in order to limit the membrane surface. The CO_2 separated by this membrane (stream #14) is then treated and made ready for transport and storage after being taken to 110 bar (#15) in

an intercooled compression train. To meet the standards on CO_2 purity for pipeline transport and storage, if the overall concentration of non-condensable gases in the separated CO_2 flow exceeds the assumed specifications of 4% (de Visser et al., 2008), a self-refrigerated two-stage phase-change CO_2 purification unit (CPU) is adopted. The vent gas from the flash units (#16), which contains most of the non-condensable gases but also has a significant concentration of CO_2, is recycled to the CCM inlet so as to reduce the CO_2 lost in the purification process. In the CCM, it is assumed that about 90% of the CO_2 generated by NG combustion is separated.

The second membrane is the CO_2 recycle membrane (CRM). It is a 4-port membrane with a counter-current arrangement where the retentate of the CCM represents the feed stream (#11) while fresh air (#2) is used as sweep gas on the permeate side before entering the GT compressor. The idea of adopting a selective CO_2 recycle through this CRM is to substitute the large air excess needed in a GT to control the maximum cycle temperature with recirculated CO_2. In this way, dilution of CO_2 in the flue gas with nitrogen and oxygen is reduced with beneficial effects on the CO_2 partial pressure in the CCM. In the CRM, the flow rate of the separated CO_2 is determined to obtain the target Turbine Inlet Temperature (TIT) of 1360°C in the gas turbine engine. The flow rate of fresh air, used as sweep gas in the CRM, is adjusted to obtain an O_2 concentration of 2.5%vol. at the combustor outlet (#6), to guarantee a complete combustion.

A flue gas compressor is used to increase the pressure of the feed gas to the two membranes and increase the driving force for separation. In the base case, a feed pressure of 2 bar has been assumed. A turbine is then used to recover the pressure energy from the retentate of the CRM (#12).

The pressure drop in the two membrane stages is assumed equal to 2.5% of the feed inlet pressure. It is hence assumed that the geometry of the membranes is adapted in each case to achieve the target pressure drop, as discussed in the following sections. Nearly atmospheric pressure is always kept on the permeate side of the CRM. A fan is used on the fresh air stream to balance the ~7% total pressure drop assumed in the filter, the membrane and the downstream gas cooler. A gas cooler is used to cool the permeate stream of the CRM (#3) to the GT compressor inlet temperature of 30°C (#4). Such cooling is needed due to the heat transfer in the CRM and the relatively high temperature of the gas permeating through the membrane, as a result of the higher temperature of the feed stream (#11) after flue gas compression.

The gas turbine is calculated considering a pressure ratio of 18.1 and a TIT of 1360°C, in line with the state of the art of large scale heavy duty GTs (EBTF, 2011). It must be highlighted that it is unlikely that commercial GTs can be adapted for operating under the conditions imposed on this plant, because the increase in CO_2 concentration of the GT working fluid (25-30% vol. at the compressor inlet) leads to modified properties of the working fluid, affecting the fluid-dynamics of the turbomachines (especially critical in the compressor) and the heat transfer in the turbine cooled blades. Therefore, the geometry of commercial GT compressor and turbine will need to be redesigned for this application. The combustor will also require a substantial redesign to achieve complete combustion of the fuel with an oxidant stream with a relatively low O_2 content. As a term of comparison, a minimum O_2 concentration of 17.8% at the inlet of a GE gas turbine combustor was found to be acceptable for a stable and efficient combustion (ElKady et al., 2009; Evulet et al., 2009), to be compared with about 14% of the base case of this study.

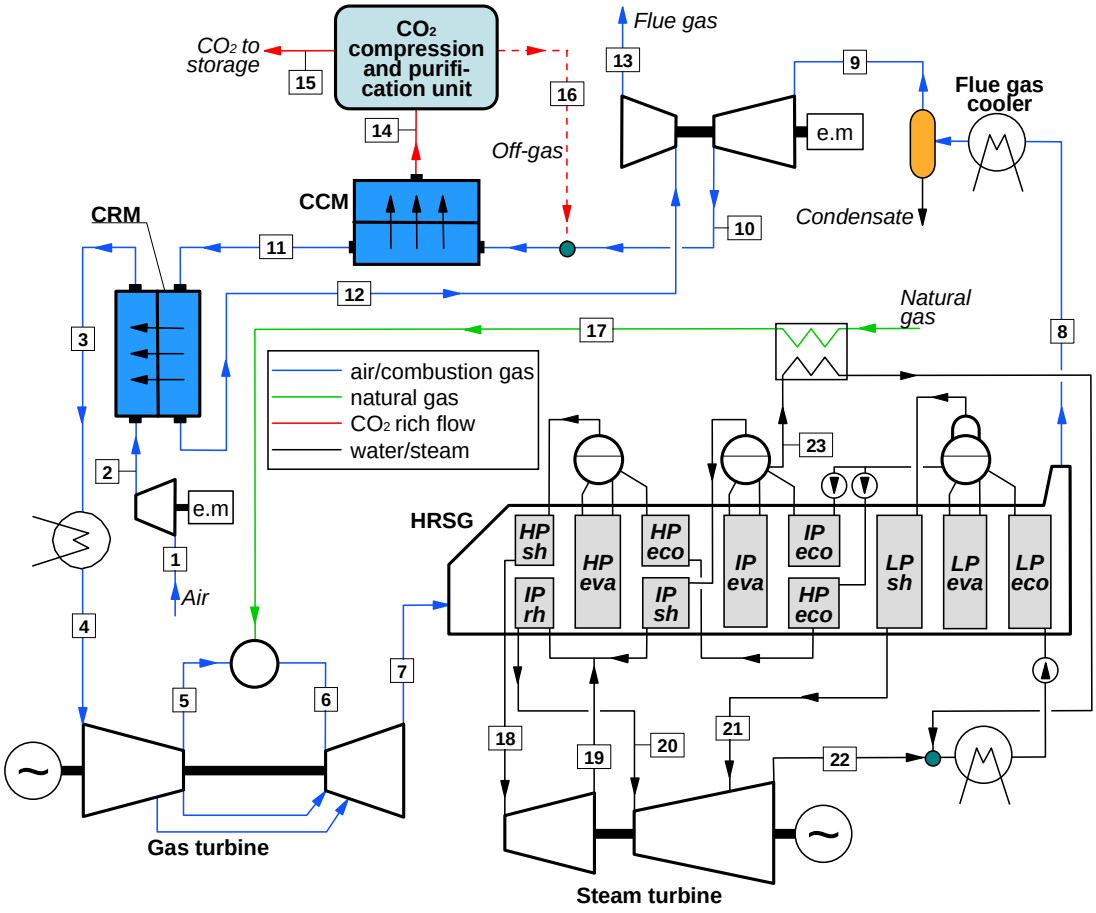

Figure 1 Process configuration of the NGCC power plant with CO_2 membranes assessed in this work.

In this work, the gas turbine is calculated with the model presented in (Chiesa and Macchi, 2004), by considering a machine design tailored for this application, but with the same technological level of today's gas turbines, i.e. keeping the current cooling performance of the benchmark GT cycle with no gas recycle. The gas turbine model reliably predicts the performance of the cooled expansion, by calculating the coolant flow rate and the stage efficiency as a function of the thermodynamic and transport properties of the gas that flows in the machine. The heat recovery steam cycle is based on a conventional three pressure level HRSG with reheat (130/28/4 bar, 565/565/300°C).

All the main assumptions for the power cycle are reported in Table 1. A constant fuel input of 711 MWLHV is assumed in all the cases, as estimated for the benchmark NGCC without capture. Mass and energy balances are solved with the in-house code GS (GECOS, 2016), developed at the Department of Energy of Politecnico di Milano, except CO_2 compression, purification and membrane separation, for which Aspen Plus V8.4® and Aspen Custom Modeler ("Aspen Technolgy, Inc.," 2013) have been used.

Table 1 Main assumptions used for simulations.

NATURAL GAS	
Molar composition, %	
CH_4, C_2H_6, C_3H_8, C_4H_{10}, CO_2, N_2	89, 7, 1, 0.1, 2, 0.9
Lower Heating Value, MJ/kg	46.48
Higher Heating Value, MJ/kg	51.45
CO_2 emission factor, g_{CO2}/MJ_{LHV}	56.99
GAS TURBINE	
Compressor pressure ratio	18.1*
TIT (total temperature at first rotor inlet), °C	1360
Compressor polytropic efficiency, %	92.5
Turbine cooled stage isentropic efficiency, %	92.1**
Turbine uncooled stage isentropic efficiency, %	93.1**
Air pressure loss in the combustor, %	3
Temperature of fuel to combustor, °C	160
Shaft mechanical efficiency, %	99.6
Generator electrical efficiency, %	98.5
STEAM CYCLE	
Evaporation pressure levels, bar	130/28/4
Maximum SH/RH steam temperature, °C	565
Minimum approach point ΔT in SH/RH, °C	25
Pinch point ΔT in HRSG, °C	10
Liquid subcooling ΔT at drum inlet, °C	5
Heat losses, % of heat transferred	0.7
Gas side pressure loss in HRSG, kPa	3
HP SH pressure loss, %	7
HP/IP pumps hydraulic efficiency, %	85/75
HP/IP/LP turbine isentropic efficiency, %	92/94/88
Turbine shaft mechanical efficiency, %	99.6
Generator electrical efficiency, %	98.5
Condensing pressure, bar	0.048
FLUE GAS COMPRESSOR AND EXPANDER	
Compressor pressure ratio	2*
Compressor polytropic efficiency, %	85
Expander polytropic efficiency, %	90
Mechanical/electrical efficiency, %	93
CO_2 PURIFICATION AND COMPRESSION	
Low temperature flash temperature, °C	-56
High temperature flash temperature, °C	-42
Pressure at LT flash inlet, bar	32.6
Minimum ΔT in low temperature heat exchangers, °C	3
Number of intercooled compression stages	5
Isentropic efficiency, %	85
Mechanical/electrical efficiency, %	92.2
Inter-coolers outlet temperature, °C	28
Inter-coolers pressure losses, %	2
Liquid CO_2 temperature at pump inlet, °C	25
Liquid CO_2 pressure at pump inlet, bar	98
CO_2 VACUUM PUMP	
Gas pressure at vacuum pump inlet, bar	0.2*
Number of inter-cooled stages	3
Isentropic efficiency, %	85
Mechanical/electrical efficiency, %	92.2
Inter-coolers outlet temperature, °C	28

* Base case values. Variables subject to sensitivity analysis.

** Values for large turbine stages. The actual efficiency of each stage is corrected by taking scale effect into account (Chiesa and Macchi, 2004).

2.2 Membrane model

The first step in evaluating the membrane area involves defining the module dimensions and geometry. One of the most relevant aspects is the surface area to volume ratio (s/v), which affects both the thermal and the fluid-dynamic problems. In general, a low value of s/v corresponds to lower pressure drop and a bigger module for a given separation efficiency. Commercial modules of polymeric membranes are usually spiral wound or hollow fiber. The first have a moderate s/v with relatively low pressure drop. Hollow fibers have a very large s/v and the pressure drops in the fiber lumen can be significant. Moreover, the shell side needs to be carefully designed to avoid flow maldistribution. In this paper, reference is made to the spiral wound arrangement adopted in membrane modules considered in the DOE funded project n. FE0005795 (DOE/NETL, 2010).

In the spiral-wound configuration, the module consists of some membrane sheets wound around a central collection/distribution pipe. Spacers interposed among the membrane sheets form the channels that allow the streams flowing on the feed and permeate side. This arrangement is suitable for use in both 3-port and 4-port modules. The cross section of a 4-port module is shown in Figure 2. The feed streams flows axially through the module (i.e. in a direction perpendicular to the cross section). The sweep stream is distributed by the central pipes and flows through the spiral-shaped channels towards the periphery of the module where it is collected in an outlet manifold. Even though this assembling approach produces a cross-flow configuration on the single module, a counter-current membrane can be obtained by placing more modules in series as shown in Figure 3. In the presence of a sweep gas, a counter-current configuration allows the required membrane area to be decreased thanks to its favourable partial pressure profile. The CRM of plant in Figure 1 is arranged in this way.

The CCM membrane has instead a 3-port configuration given that sweep gas is avoided to prevent the dilution of the separated CO_2. In the 3-port configuration, the feed stream flows exactly the same way as in the 4-port. The permeate gas flows inward and is collected in the inner pipe. Without a sweep gas, a 0.2 bar permeate pressure is kept in order to reduce the membrane area and post compression of the gas is required.

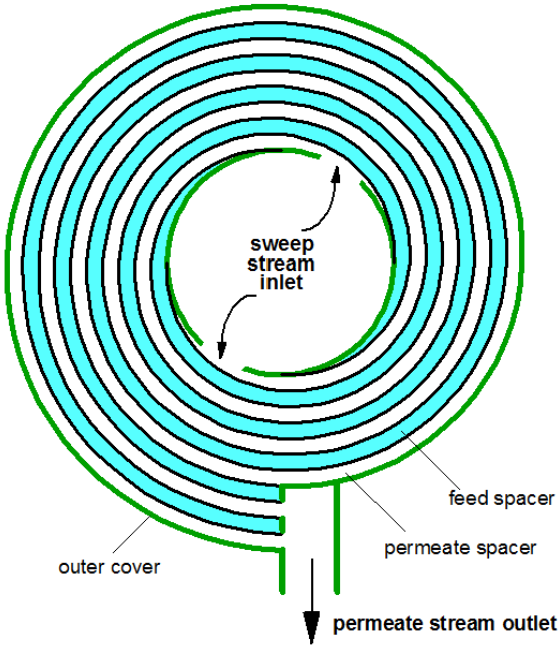

Figure 2 Cross section of the 4-port spiral wound module considered in the paper. In this sketch, four membranes sheets are wound around the central distribution pipe.

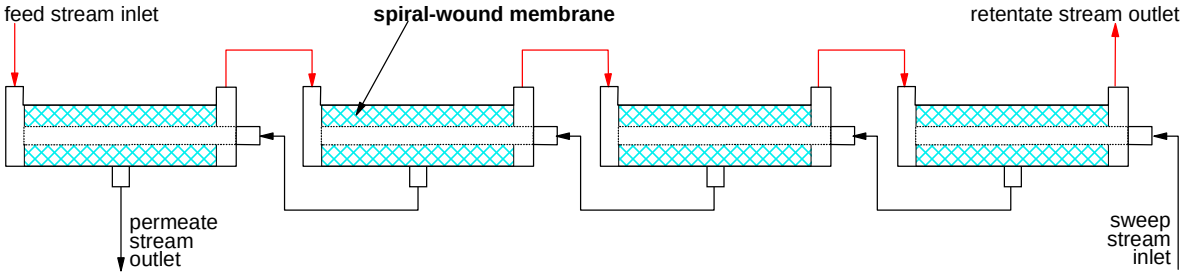

Figure 3 String of 4-port modules connected in series in counter-current configuration.

The model used in this study to evaluate the membrane performance, simulates the spiral wound modules connected in series as a planar counter-current membrane. The membrane is then discretized along the axial coordinate according to the schematic shown in Figure 3 and a finite difference method implemented in Aspen Custom Modeler® is applied to solve the conservation, heat and mass transfer equations.

2.2.1 Modelling mass conservation and mass transfer.

Permeation through the polymeric membrane is described through Eq. 1 that is derived from the solution-diffusion model. In this representation, the flux (J) (flow rate per unit of time per unit of membrane area) of the gas species i is proportional to the difference in partial pressures ($p \cdot x_{i,int}$) at the gas-membrane interface on the two sides of the membrane through the permeance (K_i).

$$J_i = K_i \cdot \left(p_{feed} \cdot x_{i,feed,int} - p_{perm} \cdot x_{i,perm,int}\right) \quad \text{Eq. 1}$$

Permeance is evaluated from literature data, assuming that the support and inter-diffusive layer do not pose any additional resistance to permeation.

By neglecting the axial diffusion effects, the steady state mass conservation equation is then written for both the feed and the permeate side for the k-th cell along the axial coordinate and for each i-th species included in the streams.

$$j_i^k = \left(\dot{n}_i^{(k-1)} - \dot{n}_i^{(k)}\right) \quad \text{Eq. 2}$$

The previous equations 1-2 are linked by Eq.3:

$$j_i^k = J_i^k \cdot \Delta S_k \quad \text{Eq. 3}$$

Fick's law of diffusion is used to relate the concentration gradient from the bulk phase (used to defined molar flow rates in eq.2) to the interface (considered in eq. 1). The binary diffusion coefficients are evaluated by the Aspen routines for thermo-physical properties.

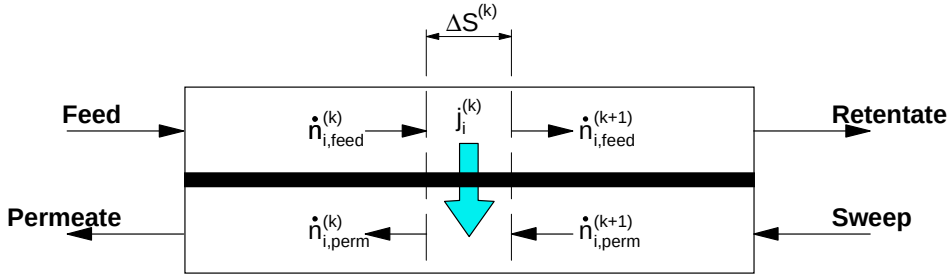

Figure 4 Axial discretization of the membrane module

2.2.2 Fluid-dynamics modelling

One of the most important aspects in the simulation of a membrane module is the pressure loss. In the literature (Pfaff and Kather, 2009; van Hassel, 2004), pressure drop along the membrane is often neglected or assumed to be a fixed value. However, calculation of pressure loss is essential for a proper evaluation of the efficiency of the power plant in which the membrane is integrated (Brinkmann et al., 2015). The pressure profile is also crucial for the permeation driving force and has a strong effect on the CO_2 flux across the membrane, influencing its area. Neglecting the pressure drop entails an overestimation of the membrane separation efficiency if the pressure of the feed and the permeate streams ($p_{feed,IN}$ and $p_{perm,OUT}$) is fixed. The model accounts for the pressure losses due to the flow inside the channels, evaluated by the classical correlations that are valid for laminar flow. Contributions to pressure loss due to inlet and outlet headers and interconnections between modules are neglected. However, pressure drops depend on the geometry of the membrane. Evaluating the actual geometry of the modules and their overall number is beyond the scope of this paper. Pressure losses are therefore evaluated by assigning the overall length of

the membrane channels (i.e. considering all the modules in series). A channel length of 4 m is assumed as a first guess, while the height of the channels is adjusted to obtain the target pressure loss of 2.5% on the feed side of both membranes and of 5.6% on the permeate side of the CRM. The velocity of the stream is constrained to a maximum of 10 m/s. If higher velocities are obtained, a shorter membrane length is assumed resulting in a lower pressure drop.

2.2.3 Thermal balance modelling

The model also solves the energy balance of the membrane to assess the heat exchange between the feed and the sweep streams. Temperature profiles do not actually affect mass transfer evaluated by the model, provided that temperature dependent functions are not used for permeance. It is however important to solve the thermal balance to verify that temperature is always above the water dew point so that water condensation does not occur inside the channels. Solving the energy balance of the membrane is also important for calculating the gas outlet temperatures from the CRM, that affect the power plant heat balance and cooling duty.

Heat transfer between the streams has been evaluated using the following assumptions:

- Convective heat transfer coefficients for laminar flow along the channels are evaluated by fixed values of the Nusselt number derived from (Incropera and De Witt, 2002) according to the shape factor of the channel, characterized by a rectangular cross section.
- Conduction across the membrane wall is evaluated assuming a thermal conductivity of the material of 0.35 W/m-K and a thickness of 5 μm (Huang et al., 2008).
- Axial conductivity along the membrane and heat dispersion to the outside environment are neglected.

2.3 Economic model

The economic analysis has been performed following CO2CRC methodology (Ho et al., 2008). The main assumptions for the economic analysis and the methodology for the calculation of the capital cost are shown in Table 2 and Table 4. The total capital costs are calculated as shown in Table 4. For the membrane, a cost of 50 US$/m^2 has been assumed (Merkel et al., 2010) independent of the type of membrane considered. For the gas turbine, HRSG and steam cycle, the EBTF cost functions from (EBTF, 2011) have been used, corrected to US$2015 using the CEPCI annual index (556.8) and currency conversion for €/$ based on average 2008 values (€/$=1.47) (Eq. 4) (DOE/NETL, 2013). For the GT, a 20% additional cost has been assumed for the plants with selective flue gas recycle to take into account the costs for potential additional cost of machines operating with CO_2-enriched gas. For the other components an exponential correlation has been adopted.

$$Capex = \frac{CEPCI\ (2015)}{CEPCI\ (2008)}\ C_0 \left(\frac{S}{S_0}\right)^{SF} \qquad \text{Eq. 4}$$

The assumed price of electricity, needed in the CO2CRC methodology to price the effect of different power outputs of the plants with capture, is 58.8 US$/MWh. This value corresponds to the cost of electricity obtained for the reference NGCC without capture with a fuel price of 7 US$/GJ.

Table 2 Equipment cost assumptions and references for the plant components.

Plant Component	Scaling Parameter (sp)	Reference Bare Erected Cost C_0 (M$2015)	Reference Size, S_0	Scale factor (sf)
Power section				
Gas turbine, generator and auxiliaries (EBTF, 2011)	GT Net Power, MW	70.3	272	0.67
HRSG, ducting and stack (EBTF, 2011)	U*A, MW/K	46.4	12.9	0.67
Steam turbine, generator and auxiliaries (EBTF, 2011)	ST Gross Power, MW	48.0	200	0.67
Cooling water system and BOP (EBTF, 2011)	Condenser cooling duty, MW	70.6	470	0.67
Gas conditioning and CO_2 separation section				
Air Blower (Allinson et al., 2006)	Flow, m^3/s	0.54	160	1
Flue gas Compressor/Expander (Allinson et al., 2006)	Power, MW	43.1	1	0.79
Vacuum pump (Allinson et al., 2006)	Inlet flow, m^3/s	1.04	70	1
CO_2 compressor (Allinson et al., 2006)	Power, MW	47.4	1	0.79
Membrane Housing (Allinson et al., 2006)	10^6 m^2	0.25	0.002	0.7
Membrane	10^6 m^2	50	1	1
MEA (EBTF, 2011)	kg/s CO_2 captured	124	50.8	0.8

Table 3 Main assumptions for the economic analysis

Currency	US$2015
Discount rate	7 % (real)
Project life	25 years
Construction period	2 years
Plant load factor	90%
Price of electricity	58.8 $/MWh
Price of natural gas	7 $/GJ
General and maintenance cost	6% Capex/year
Cooling water price	0.025 $/$m^3$
Expected membrane life	3 years

Table 4 Capex calculation methodology

Name	Parameter	Value
A	Process equipment cost (PEC)	Sum of all equipment cost
B	General cost	30% PEC
C	Total equipment cost (TEC)	A + B
D	Instrumentation	15% TEC
E	Electrical	7% TEC
F	Piping	20% TEC
G	Total installed cost (TIC)	A+B+D+E+F
H	Set-up cost	8% TIC
I	Engineering	5% TIC
L	Owners cost	7% (G+H+I)
M	Engineering, procurement, construction and owner's cost (EPCO)	G+H+I+L
N	Contingency	10% EPCO
O	Total capital cost (CAPEX)	M+N

2.4 Case studies

In this work the application of the three different types of membrane in Table 5 has been considered in order to investigate the effect of selectivity and permeability on the complete process. The first membrane has performance corresponding to a Polaris membrane by Membrane Technology & Research (MTR), which represents the state of the art of commercial membranes for CO_2 gas separation. The second membrane has performance corresponding to the targets set by the US Department of Energy (DOE targets) in their research programme (DOE/NETL, 2012a) and

is representative of a membrane with very high permeability (3.5 times the Polaris membrane) but relatively low selectivity. This target has not been reached yet but materials development in polymers of intrinsic micro porosity (PIMs) (Bushell et al., 2013) and thermally rearranged polymer (Choi et al., 2010) show promising progress. The third membrane has been reported in (Huang et al., 2008) and is a facilitated transport membrane. In this case, CO_2 interacts with specific sites in the polymer in the presence of water while the N_2 does not. As a consequence, the material has a very high selectivity but a lower permeability than the DOE target.

Table 5 Membrane permeance [1 GPU = 10^{-6} cm^3 (STP)/(cm^2 s cm_{Hg})] and selectivity.

Membrane Technology	Permeance (GPU)	Selectivity respect to CO_2			
		Ar	H_2O	N_2	O_2
Polaris (Merkel et al., 2010)	1000	5	0.3	50	5
DOE (DOE/NETL, 2012a)	3500	35	0.7	35	35
Huang (Huang et al., 2008)	1200	75	1	500	75

Usually, process integration studies are performed considering only one type of membrane. However, the combination of membranes with different selectivity and permeability at different locations within the same plant can be beneficial. In this paper, the three membranes have been assessed in different combinations for the CCM and CRM. In particular, Polaris and DOE membranes have been considered for both the CCM and CRM, while the Huang membrane has been considered as the CCM, in combination with either DOE or Polaris CRM.

In addition to the baseline case studies, this paper also undertakes sensitivity analysis by varying the following design parameters: (i) membranes feed pressure, by varying the flue gas compressor pressure ratio, (ii) CCM vacuum pressure, (iii) GT pressure ratio. In addition to these technical parameters, a sensitivity analysis on the price of electricity has also been performed, by increasing it to 90 US$/MWh, which is equivalent to increasing the gas price to 12 US$/GJ.

3 Discussion

3.1 Thermodynamic analysis

Table 6 to Table 9 show the main characteristics estimated for the membrane modules and the mass balances of the key steams in Figure 1 with different combinations of membranes.

Table 6 and Table 8 provide data for the cases where the DOE and Polaris membranes are used for both the CCM and CRM respectively. The results show that the material balance is similar for these two membranes, with differences mainly observed in the CO_2 concentration of the feed to each membrane unit, which is higher for the DOE membrane (28.2% vs. 25.3% at the CCM inlet). This happens despite the lower selectivity of the DOE membrane towards nitrogen. Its higher selectivity towards oxygen causes a lower back diffusion of oxygen from the sweep side to the feed side in the CRM. In contrast, because of the higher oxygen back diffusion, in the Polaris membrane case a larger flow rate of air is needed to provide the oxygen required for the combustion in the GT (439 kg/s vs. 394 kg/s), causing a larger nitrogen input into the gas turbine cycle fluid. With both the Polaris and DOE membrane cases in Table 6 and Table 8, further CO_2 purification before compression is required due to the

relatively low selectivity. In these baseline conditions investigated, the CO_2 separated in the CCM (stream #14) has a purity between 88 and 91%mol. (dry basis).

In Table 7 and Table 9, the DOE and Polaris membranes are used in the CRM while the Huang-type membrane is used in the CCM. In these cases, the high selectivity of the Huang-type membrane produces a high purity CO_2 (between 96.8 and 98.6%), not requiring any further CO_2 purification step to meet the purity specifications assumed in this paper.

In all the cases, it can be observed that the CRM needs a membrane area one order of magnitude higher than the CCM. This is mainly due to the much larger CO_2 flow rate to be separated in the CRM (between 4.0 and 4.5 kmol/s, depending on the specific case) with respect to the CCM (0.83-0.86 kmol/s). For a fixed feed and permeate pressure, the membrane area is strictly linked to the permeability. Therefore, when the DOE membrane is used, its surface area is about 70% smaller than the corresponding Polaris and Huang membranes.

Table 6 Membrane module characteristics and properties of the significant streams for the use of a DOE membrane as the CCM and CRM.

Membrane module characteristics										
						CCM			CRM	
Membrane						DOE			DOE	
Surface, $m^2 \times 10^3$						20.9			372.8	
Channel length [m]						0.9			4	
Feed channel:	height [mm]					1.5			1.1	
	maximum velocity [m/s]					10.1			4,5	
	maximum Reynolds number					1386			293	
	pressure loss, %					2.5			2.5	
Permeate channel:	height [mm]					1.3			1.4	
	maximum velocity [m/s]					5.2			2.6	
	maximum Reynolds number					107			320	
	pressure loss, %					3.8			5.6	

Stream properties										
	T	P	G	W	Q	Composition (%mol.)				
Stream no.	°C	bar	kg/s	kg/kmol	kmol/s	Ar	CO_2	H_2O	N_2	O_2
2	40	1.07	393.9	28.851	13.654	0.92	0.03	1.03	77.28	20.73
3	95	1.01	629.2	31.778	19.800	0.64	22.51	4.67	58.27	13.91
10	107	2.03	615.8	32.248	19.095	0.66	28.16	5.55	60.46	5.17
11	107	1.98	574.9	31.873	18.036	0.70	25.22	4.75	63.89	5.45
12	40	1.93	339.6	28.561	11.89	1.06	0.80	0.61	88.62	8.91
14	107	0.20	43.6	38.189	1.142	0.00	74.59	17.8	7.01	0.60
15	25	110	37.3	43.520	0.857	0.00	96.82	0.00	2.80	0.38
16	32	2.1	2.68	32.449	0.083	0.00	26.62	0.00	68.95	4.42

Table 7 Properties of the significant streams for the use of Huang and DOE membranes in the CCM and CRM respectively.

Membrane module characteristics										
						CCM			CRM	
Membrane						Huang			DOE	
Surface, $m^2 \times 10^3$						60.7			387.9	
Channel length [m]						4.0			4.0	
Feed channel:	height [mm]					2.4			1.1	
	maximum velocity [m/s]					8.0			2.5	
	maximum Reynolds number					2065			291	
	pressure loss, %					2.5			2.5	
Permeate channel:	height [mm]					2.1			1.4	
	maximum velocity [m/s]					5.2			5.0	
	maximum Reynolds number					146			317	
	pressure loss, %					9.5			5.6	

Stream properties										
	T	P	G	W	Q	Composition (%mol.)				
Stream no.	°C	bar	kg/s	kg/kmol	kmol/s	Ar	CO_2	H_2O	N_2	O_2
2	40	1.07	386.0	28.851	13.378	0.92	0.03	1.03	77.28	20.73
3	95	1.01	628.1	31.771	19.771	0.62	22.64	4.93	57.89	13.92
10	107	2.03	613.8	32.283	19.012	0.65	28.39	5.55	60.24	5.18
11	107	1.98	574.0	31.874	18.009	0.68	25.36	4.95	63.56	5.45
12	40	1.93	331.9	28.567	11.617	1.06	0.82	0.48	89.01	8.63
14	107	0.20	39.7	39.636	1.002	0.00	82.75	16.2	0.61	0.34
15	25	110	36.8	43.844	0.839	0.00	98.86	0.00	0.73	0.41
16	-	-	-	-	-	-	-	-	-	-

Table 8 Properties of the significant streams for the use of a Polaris membrane as the CCM and CRM.

Membrane modules characteristics			
		CCM	CRM
Membrane		Polaris	Polaris
Surface, $m^2 \times 10^3$		73.4	1237
Channel length [m]		4.0	4.0
Feed channel:	height [mm]	2.4	0.8
	maximum velocity [m/s]	7.1	1.2
	maximum Reynolds number	1641	65
	pressure loss, %	2.5	2.5
Permeate channel:	height [mm]	2.4	0.9
	maximum velocity [m/s]	4.6	2.2
	maximum Reynolds number	135	99
	pressure loss, %	6.8	5.6

Stream properties

	T	P	G	W	Q	Composition (%mol.)				
Stream no.	°C	bar	kg/s	kg/kmol	kmol/s	Ar	CO_2	H_2O	N_2	O_2
2	40	1.07	439.1	28.851	15.219	0.92	0.03	1.03	77.28	20.73
3	102	1.01	636.0	31.437	20.230	0.69	20.01	4.06	61.55	13.68
10	108	2.03	625.0	31.790	19.660	0.71	25.28	5.55	63.38	5.09
11	108	1.98	581.0	31.507	18.441	0.76	22.45	4.00	67.48	5.32
12	40	1.93	384.1	28.603	13.430	1.04	0.71	0.54	87.52	10.18
14	108	0.20	47.5	35.848	1.326	0.00	64.74	26.7	4.88	3.68
15	25	110	37.6	43.452	0.865	0.00	95.95	0.00	1.80	2.25
16	31.9	2.1	3.58	33.39	0.11	0.00	26.81	0.00	45.88	27.31

Table 9 Properties of the significant streams for the use of Huang and Polaris membranes in the CCM and CRM respectively.

Membrane module characteristics			
		CCM	CRM
Membrane		Huang	Polaris
Surface, $m^2 \times 10^3$		70.9	1340
Channel length [m]		4.0	4.0
Feed channel:	height [mm]	2.4	0.7
	maximum velocity [m/s]	7.1	1.1
	maximum Reynolds number	1714	83
	pressure loss, %	2.5	2.5
Permeate channel:	height [mm]	1.6	0.9
	maximum velocity [m/s]	5.8	2.0
	maximum Reynolds number	122	92
	pressure loss, %	16.5	5.6

Stream properties

	T	P	G	W	Q	Composition (%mol.)				
Stream no.	°C	bar	kg/s	kg/kmol	kmol/s	Ar	CO_2	H_2O	N_2	O_2
2	40	1.07	430	28.851	14.907	0.92	0.03	1.03	77.28	20.73
3	95	1.01	633	31.366	20.175	0.68	20.09	4.90	60.62	13.71
10	108	2.03	619	31.844	19.425	0.71	25.61	5.55	63.00	5.13
11	108	1.98	578	31.434	18.403	0.75	22.53	4.87	66.46	5.40
12	40	1.93	376	28.607	13.134	1.05	0.73	0.48	87.71	10.04
14	108	0.20	40.1	39.244	1.022	0.00	81.18	17.7	0.73	0.39
15	25	110	36.8	43.812	0.841	0.00	98.64	0.00	0.88	0.48
16	-	-	-	-	-	-	-	-	-	-

In Table 10, the energy balance and the main overall performance indexes of these four cases are shown in the 3rd to 6th columns. In the last column a selected case with Huang and DOE membranes and reduced feed pressure is also reported as a significant case resulting from the sensitivity analysis presented later in this paper.

In the first two columns of Table 10, the data for the benchmark combined cycle plant without capture and with capture by post-combustion MEA absorption are also reported. For the benchmark plant with CO_2 capture, heat for MEA regeneration has been assumed to be 3.95 GJ/tonnCO_2, in agreement with (EBTF, 2011). Heat is provided by steam at 4 bar partly taken from the LP drum of the HRSG and partly bled from the steam turbine.

Focusing on the four cases with the same membrane feed pressure, the main difference in the energy balances is associated with the energy for CO_2 compression, which is lower when a Huang CCM is used due to the higher concentration of CO_2 in the permeate stream. In all cases, the main efficiency penalty is related to flue gas compression/expansion. The net electric consumption of flue gas compression and expansion ranges from about 24.9 MW_e (or 3.5 percentage points of LHV efficiency penalty) for the Polaris CRM cases to 26.2-26.4 MW_e (or 3.7 percentage points LHV) for the DOE CRM cases. The second largest energy loss is attributed to CO_2 compression (sum of the vacuum pump and the CO_2 compressors), accounting for an efficiency penalty of 2.7 percentage points LHV for the Huang CCM cases and 3.1-3.3 percentage points LHV for the DOE and Polaris CCM cases.

Table 10 Power balance for different membrane technologies and comparison with a MEA benchmark.

	Reference NGCC w/o capture	Reference NGCC with MEA	CO_2 membrane cases				
CO_2 capture membrane (CCM)			DOE	Huang	Polaris	Huang	Huang
CO_2 recycle membrane (CRM)			DOE	DOE	Polaris	Polaris	DOE
CCM Feed/Permeate Pressure	-	-	2/0.2	2/0.2	2/0.2	2/0.2	1.5/0.2
CCM area, $m^2 * 10^3$	-	-	20.9	60.7	73.4	70.9	102.3
CRM area, $m^2 * 10^3$	-	-	372.8	387.9	1236.6	1340.0	690.5
Power balance, MW_e							
Gas turbine net power	272.1	272.1	248.7	248.6	250.8	250.5	248.6
Steam turbine gross power	147.1	106.8	168.9	169.0	167.1	167.4	169.0
Steam cycle pumps	-1.79	-1.79	-2.14	-2.19	-2.11	-2.11	-2.19
Auxiliaries for condenser heat rejection	-1.86	-1.87	-2.09	-2.10	-2.06	-2.09	-2.10
MEA process		-2.23					
Auxiliaries for flue gas and GT air cooling			-0.82	-0.85	-0.75	-0.83	-0.06
Fresh air fan			-3.01	-3.76	-2.36	-4.18	-2.16
Flue gas compressor		-6.86	-46.16	-45.98	-47.44	-46.89	-25.84
Flue gas expander			19.99	19.56	22.53	22.08	9.14
CO_2 vacuum pump			-6.12	-5.40	-6.71	-5.47	-5.40
CO_2 compression		-12.01	-16.20	-13.72	-16.78	-13.78	-13.71
Auxiliaries for CO_2 cooling			-0.28	-0.29	-0.34	-0.25	-0.29
Gross Power, MW_e	419.2	378.9	417.6	417.6	417.9	417.9	417.6
Net Power, MW_e	415.6	352.3	360.8	362.9	361.8	364.4	374.2
Heat input, MW_{LHV}	711.3	711.3	711.3	711.3	711.3	711.3	711.3
Net electric efficiency, $\%_{LHV}$	**58.42**	**49.53**	**50.73**	**51.02**	**50.87**	**51.23**	**52.62**
Net efficiency penalty, $\%_{LHV}$		-8.89	-7.69	-7.40	-7.55	-7.19	-5.80
Carbon capture ratio, %		91.25	90.10	90.08	90.12	90.07	90.08
Specific emission, kg/MWh	353.7	39.3	41.84	41.59	41.81	41.68	40.33
Specific emission reduction, %		88.90	88.17	88.24	88.18	88.21	88.60
SPECCA, $MJ_{LHV}/kgCO_2$		**3.52**	**3.00**	**2.86**	**2.93**	**2.77**	**2.17**
CO_2 purity, %mol (dry)		99.93	96.82	98.86	95.95	98.64	98.86

The slightly lower penalty in the Polaris CRM cases compared to the DOE CRM cases is due to the higher O_2 back-flow from the sweep to the feed side already discussed, which enhances the gas flow rate expanded in the flue

gas turbine and hence its power output. On the whole, electrical efficiencies between 50.7% and 51.2% have been obtained, with a slight advantage for the cases with Huang CCM due to the reduced consumption for CO_2 compression. As far as CO_2 emissions are concerned, the size of the CCM is adapted in each case to achieve a CO_2 capture ratio of 90% and therefore specific emissions only depend on the plant efficiency. As a result, specific emissions reductions of 88.1-88.4% have been obtained.

In Table 10 an additional case is also presented where the membrane feed pressure is reduced from 2.0 bar to 1.5 bar for the Huang membrane as the CCM and the DOE membrane as the CRM. In this case, the net flue gas compression power reduces to 17.0 MW_e, corresponding to a reduction in efficiency of 2.4 percentage points. This results in a higher net electric efficiency of 52.6%, with a penalty of 5.8 percentage points with respect to the reference NGCC without capture. The main properties of the plant streams for this case are reported in Table 11.

Table 11 Properties of the main streams of the power plant using Huang CCM and DOE CRM, with feed and permeate pressures of 1.5 and 0.2 bar respectively.

	T	P	G	Q	Molar composition (%mol.)				
Streams	°C	bar	kg/s	kmol/s	Ar	CO_2	H_2O	N_2	O_2
1	15.0	1.01	386	13.39	0.92	0.03	1.03	77.28	20.73
2	20.2	1.07	386	13.39	0.92	0.03	1.03	77.28	20.73
3	40.0	1.01	628	19.77	0.62	22.58	4.67	57.94	13.94
4	40.0	1.00	628	19.77	0.62	22.58	4.92	57.94	13.94
5	414.0	18.34	549	17.27	0.62	22.58	4.92	57.94	13.94
6	1442.6	17.79	512	16.54	0.59	26.94	15.11	54.87	2.50
7	664.5	1.01	643	20.66	0.60	26.07	13.07	55.48	4.78
8	71.2	1.01	643	20.66	0.60	26.07	13.07	55.48	4.78
9	35.0	1.01	614	19.01	0.65	28.33	5.55	60.28	5.20
10	75.7	1.52	614	19.01	0.65	28.33	5.55	60.28	5.20
11	75.7	1.48	574	18.01	0.68	25.30	4.95	63.60	5.47
12	40.6	1.44	332	11.63	1.06	0.82	0.50	88.98	8.64
13	13.6	1.01	332	11.63	1.06	0.82	0.50	88.98	8.64
14	75.7	0.20	40	1.00	0.00	82.75	16.29	0.61	0.34
15	25	110.0	37	0.84	-	98.86	-	0.73	0.41
16	-	-	-	-	-	-	-	-	-
17	160.0	68.6	15	0.85	Natural Gas (Table 1)				
18	559.51	120.9	96	5.33	-	-	100	-	-
19	337.69	28.0	96	5.33	-	-	100	-	-
20	560.95	23.0	107	5.93	-	-	100	-	-
21	32.17	0.048	114	6.35	-	-	100	-	-

The specific primary energy consumption for CO_2 avoided (SPECCA), defined in Eq. 5, can be used to provide a single index for the energy and environmental performance of plants with CO_2 capture. The values of 2.8-3.0 MJ_{LHV}/kg_{CO2} obtained for the cases with 2 bar of membrane feed pressure are better than the 3.5 MJ_{LHV}/kg_{CO2} of the benchmark plant based on MEA absorption. A significant improvement is obtained in the case with 1.5 bar feed pressure, where a low value of 2.17 MJ_{LHV}/kg_{CO2} is achieved.

$$\mathrm{SPECCA} = \frac{3600 \cdot \left({}^{1}/_{\eta} - {}^{1}/_{\eta_{ref}}\right)}{E_{ref} - E} \qquad \text{Eq. 5}$$

3.1.1 Sensitivity analysis

The most important design parameters for the system presented in this paper are the pressures on the feed side (i.e. the pressure ratio of the flue gas compressor) and the permeate pressure of the CO_2 capture membrane. The effects of these parameters on plant efficiency and membrane area are discussed in the following. In Figure 5, the effect of the CCM permeate pressure is assessed for cases with 2 bar of feed pressure. The improvement in efficiency of 0.6-0.8 percentage points with an increase in the permeate pressure from 0.2 to 0.6 bar is significant. This improvement is due to the reduction in the energy consumption of the CO_2 vacuum pump. On the other hand, the increase in the permeate pressure leads to a reduction in the driving force through the CCM and to a consequent increase in its area. This increase is particularly evident when the permeate pressure is increased from 0.4 to 0.6 bar for cases with the Huang membrane.

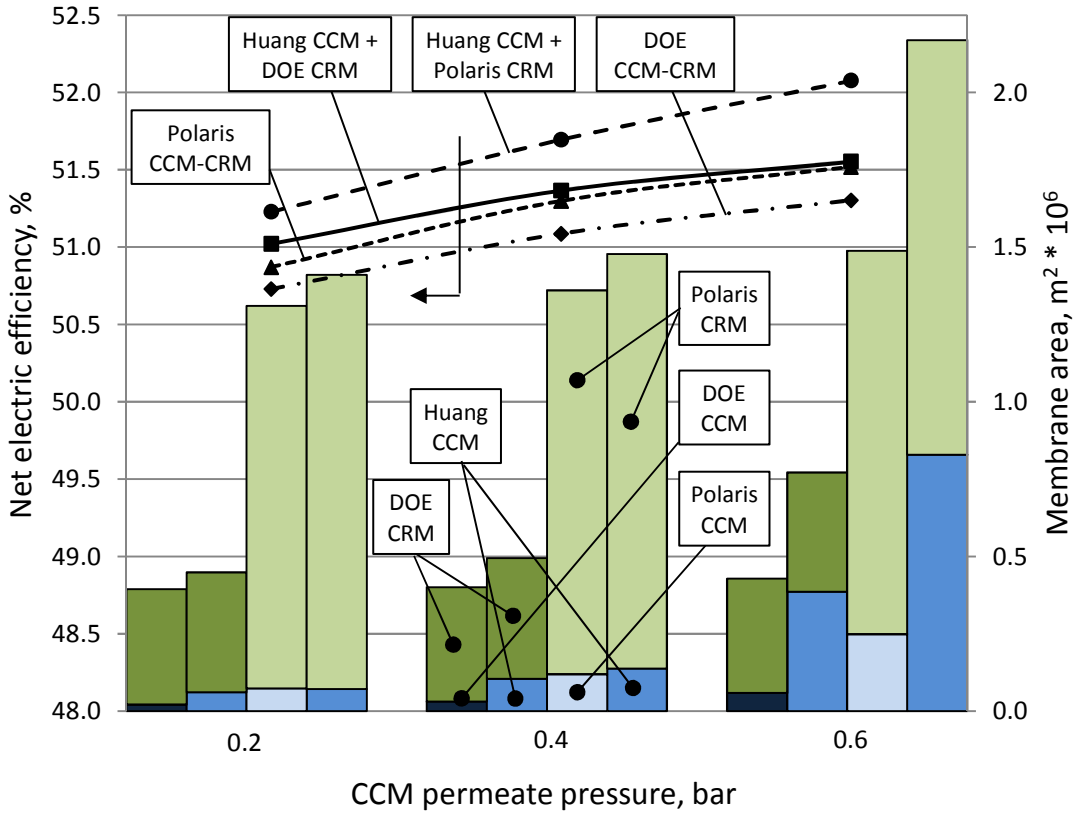

Figure 5 Effect of CCM permeate pressure on efficiency and membrane surface area for cases with 2 bar of feed pressure.

In Figure 6, the effect of flue gas pressurization on the Huang/DOE case with 0.2 bar of CCM permeate pressure is shown. The reduction of the feed pressure to 1.5 bar leads to an increase in efficiency of 1.4 percentage points. On the other hand, the area of both the CRM and CCM units increases significantly (+77% the CRM, +67% the CCM). The increase of the feed pressure to 2.5 bar reduces the plant efficiency considerably (-1.25 percentage points) but lowers the total membrane area required by -30% compared to the base case.

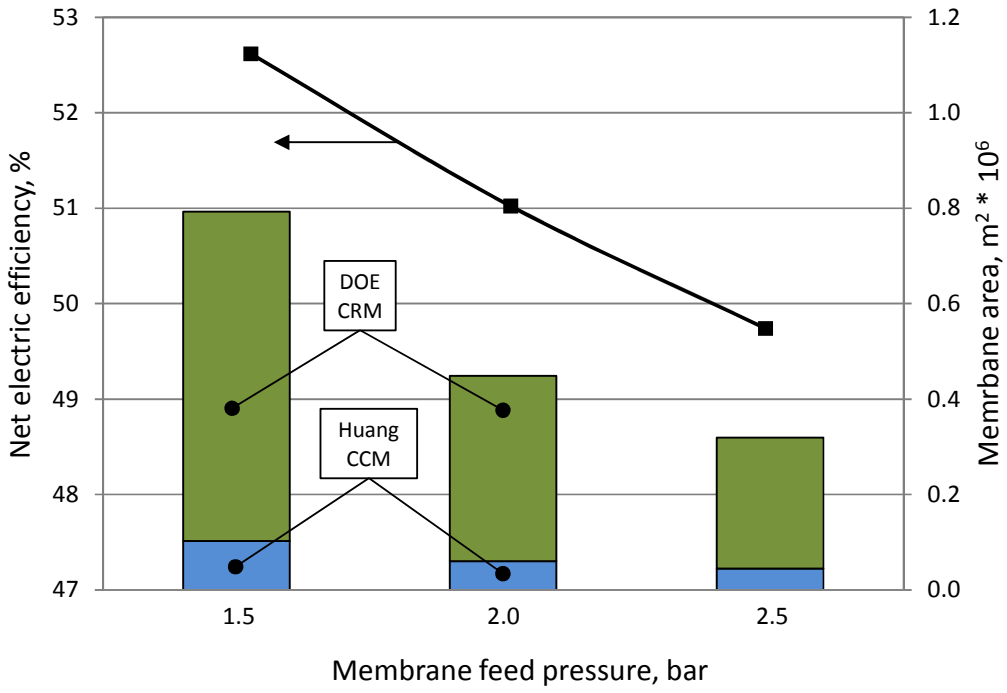

Figure 6 Effect of membrane feed pressure on efficiency and membrane area for the Huang/DOE case, CCM permeate pressure 0.2 bar.

In all the cases, the variation of feed and permeate pressures involves an opposite variation in plant efficiency and membrane area.

3.2 Economic analysis

In Figure 7, the breakdown of the equipment costs of the baseline cases in Table 10 is reported. The main difference between the membrane cases is associated with the cost of the CO_2 recycle membrane, which is much higher when the Polaris membrane is used due to the large surface area required. Of course, this result depends on the fact that for all types of membranes, the same specific cost of 50 \$/m^2 has been assumed, independently of their performance and commercial maturity. In all the cases, the cost of the CRM is much higher than the cost of the CCM, reflecting the result obtained for the membranes area. The main contribution to the investment costs is

provided by the power island, which is more expensive in the CO_2 capture cases, due to the assumed 20% increase in the GT capital cost (Capex) as a consequence of the modifications required with respect to commercial GTs in order to work with a CO_2-enriched working fluid. Another significant contribution to the capital cost is provided by the flue gas compressor and expander, whose cost is comparable (higher in the cases with DOE CRM) to the cost of the membranes. On the whole, for the cases with 2 bar of membrane feed pressure, total specific capital costs around 1550-1570 $/kW and 1330-1350 $/kW have been obtained for the Polaris CRM and the DOE CRM cases respectively. This corresponds to specific capital costs about 120-160% higher than the reference NGCC without capture and 10-25% higher than the benchmark case with CO_2 capture by MEA. The reduction of the feed pressure to 1.5 bar leads to a reduction in the specific capital cost to 1256 $/kW, i.e. about 3% more than the NGCC with MEA capture. This result is due to both the reduced cost of flue gas compressor and turbine and to the increased plant efficiency, resulting in higher net power output for the given plant size. The breakdown of the cost of electricity (COE) for the different case studies is shown in Figure 8. In all the cases, the fuel cost represents the main contribution to the COE. Due to the high membrane cost, whose effect is magnified by the cost for membrane replacement, the cases with Polaris CRM also result in the highest costs of electricity. For the cases with 2 bar of membrane feed pressure, costs of 85-86 $/MWh and 93-94 $/MWh (+45-60% and +2-12% higher than the benchmark NGCC without and with capture) are obtained for Polaris CRM and DOE CRM cases respectively.

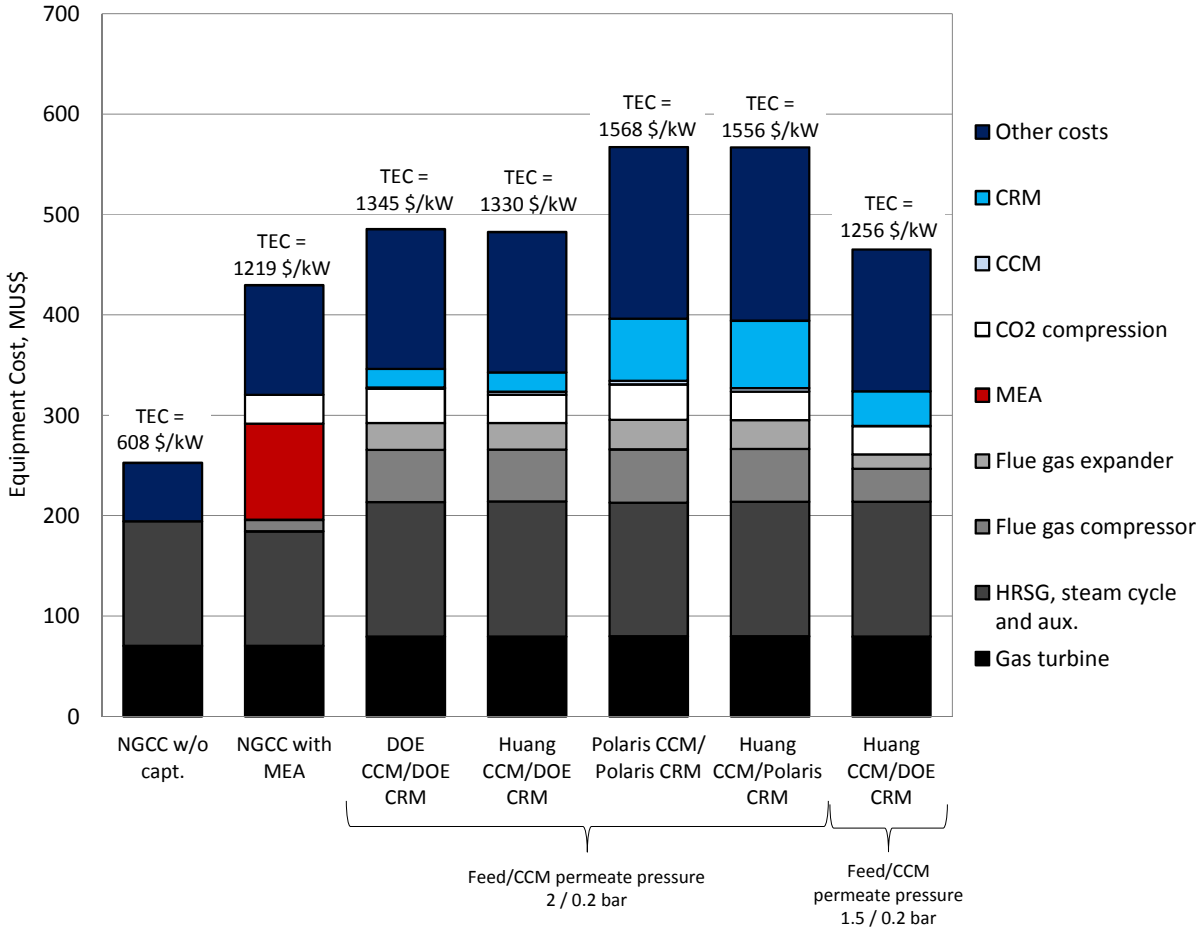

Figure 7 Breakdown of the equipment costs and total specific equipment cost.

For the case with 1.5 bar of feed pressure, the cost of electricity reduces to 82.4 $/MWh, slightly less than 83.1 $/MWh of the reference NGCC with MEA-based capture. With regard to the benchmark plants, it can be noted that the COE of the reference NGCC differs by about 1% from the one reported by NETL (DOE/NETL, 2012b) (58.8 $/MWh vs. 59.6 $/MWh), with the same share between the capital and fuel costs (22/73%). A slightly higher difference is obtained for the reference MEA case, for which a COE of 82.4 $/MWh (with Capex/fuel share of 32/60%) has been obtained in this work, compared to a COE of 90.4 $/MWh (Capex/fuel share of 30/54%) as reported by NETL (DOE/NETL, 2012b). This is mainly due to the cost for CO_2 transport and storage, which have not been included in this study and contribute for about 4 $/MWh in the NETL case.

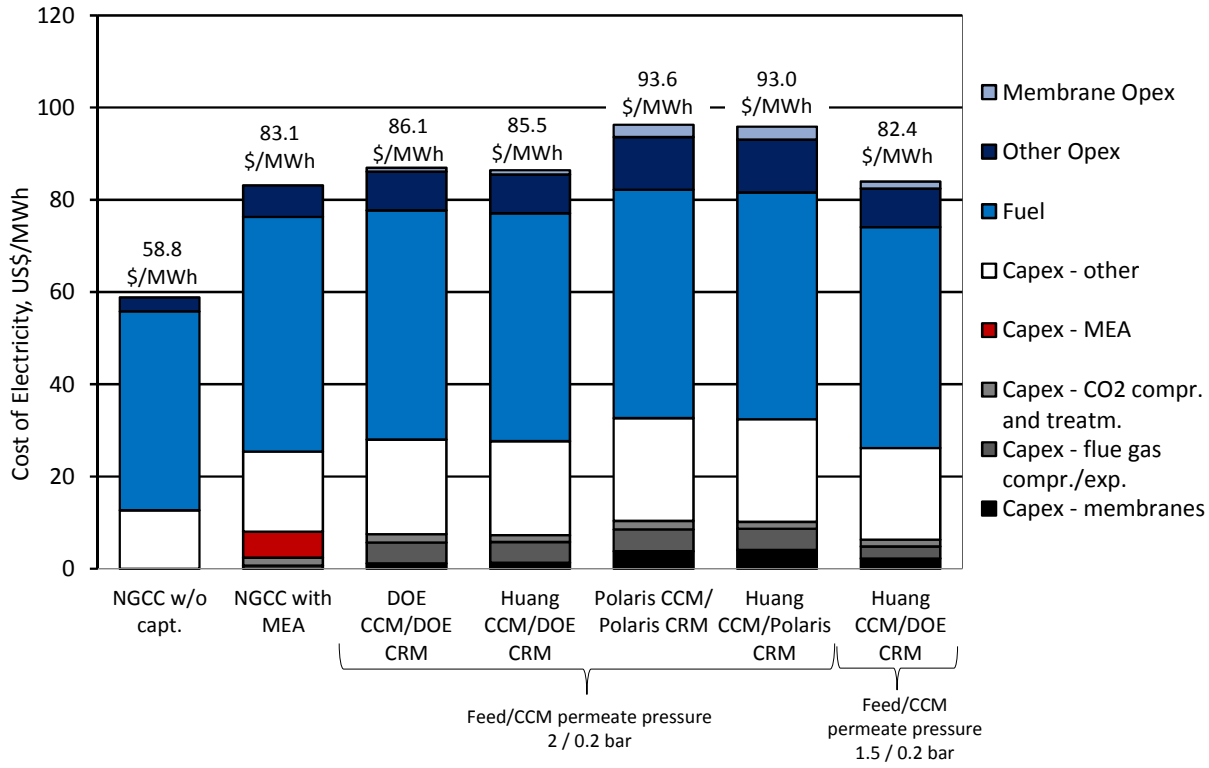

Figure 8 Breakdown of the specific cost of electricity.

The breakdown of the cost of CO_2 avoided (CCA) is shown in Figure 9. The overall trend reflects that for the COE, since all the cases are characterized by approximately the same CO_2 specific emissions. The lowest CCA, with a value of 75.4 \$/t CO_2, has been obtained for the case with Huang CCM and DOE CRM with 1.5 bar of feed pressure. This value is slightly lower than the CCA of the reference NGCC with MEA capture (77.3 $\$/t_{CO2}$). For the different membranes, the results suggest that using the DOE membrane is preferable for the CRM due to the very high permeability, while the Huang membrane is preferable as the CCM due to the high CO_2/N_2 selectivity resulting in the removal of the need for a CO_2 purification unit. It should be noted that the CCA obtained in this work for the reference NGCC is lower than those reported by NETL for the NGCC baseline case with CO_2 capture by MEA, where a cost of CO_2 avoided of 96\$/t CO_2 is reported (DOE/NETL, 2012b). This difference of about 20% in the CCA reflects the difference of ΔCOE between the reference cases with and without capture (20% as well).

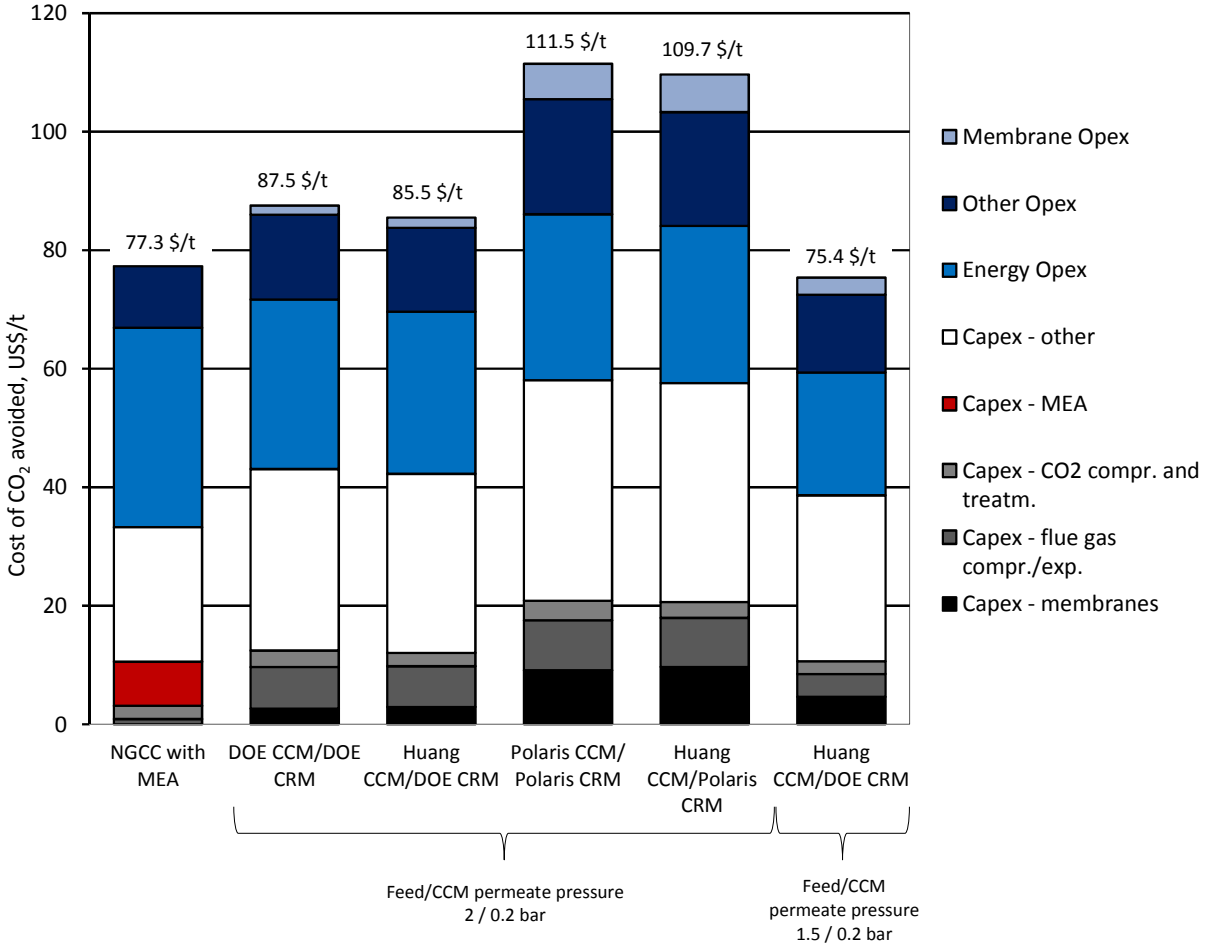

Figure 9 Effect of membrane on the cost of CO_2 avoided.

3.2.1 Sensitivity analysis

The following section provides an evaluation of the sensitivity of the cost of capture to variations in the feed and permeate pressures, increasing the price of electricity to 90 $/MWh and varying the GT pressure ratio for the Huang CCM/DOE CRM and Polaris CCM/Polaris CRM cases. The first combination appears as the most promising among the membrane technologies considered in this work. The second one is the closest to possible commercialization, being based on a commercial membrane type.

In Figure 10, plant efficiency and CCA are reported, combining different feed pressures and CCM permeate pressure. The case with the lowest cost is for the Huang/DOE membrane case with feed pressure at 1.5 bar and permeate pressure at 0.2 bar. Although reducing the feed pressure from 2.5 bar to 1.5 bar results in decreased cost, further reductions in the feed pressure to 1.1 bar did not lead to further cost savings. At 1.1 bar of feed pressure the increase in membrane area and cost offset any cost savings from the reduced cost of the flue gas compressor. For the Huang/DOE membrane case, despite the improved thermal efficiency from increasing the permeate pressure from 0.2 bar to 0.4 bar, the CCA increases for all feed pressures, especially when the feed pressure is 1.1 bar. This is

because the required membrane area at this permeate pressure is significantly large, thus the high membrane cost offsets any cost savings from the smaller vacuum pump.

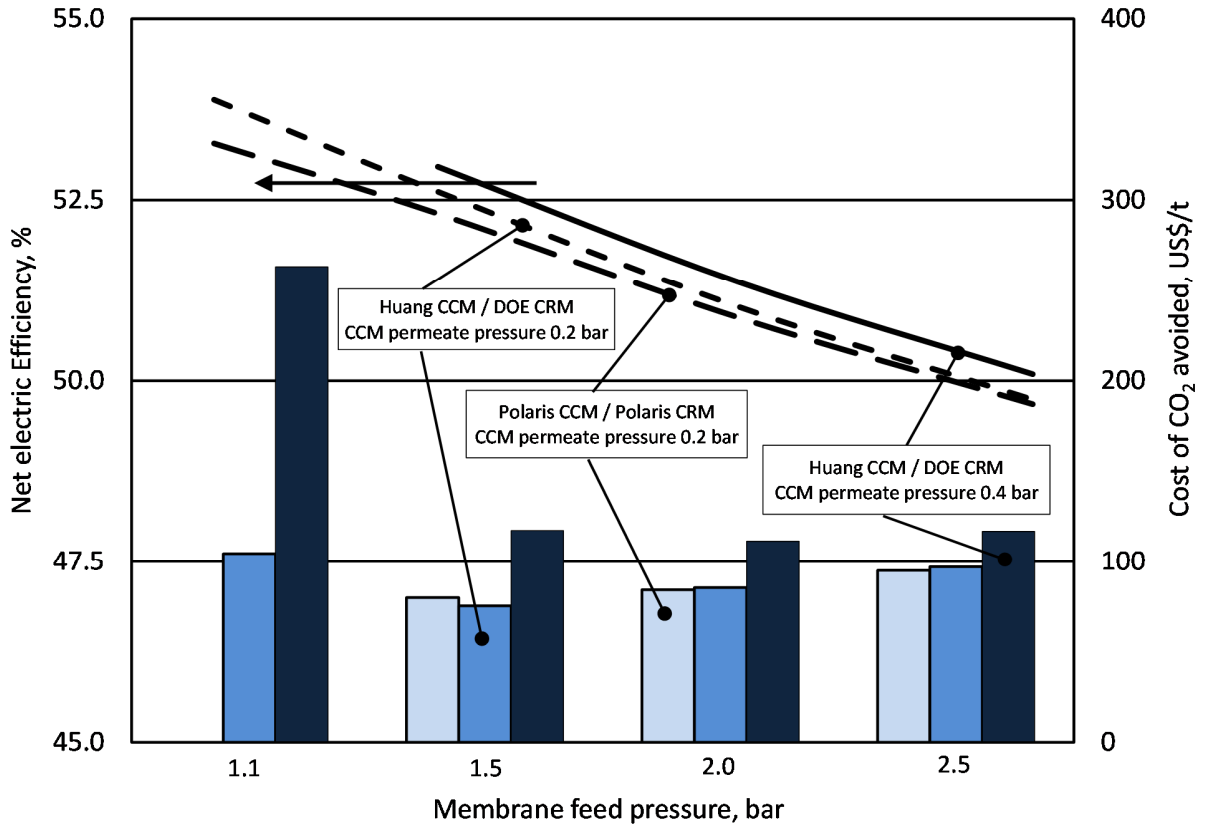

Figure 10 Cost of CO_2 avoided and electric efficiency vs. membrane feed pressure for different feed pressures and CCM permeate pressures.

In Figure 11, the effect of membrane cost and CCM permeate pressure is shown for the case with membrane feed pressure of 2 bar. For the Polaris/Polaris case, the effect of permeate pressure on the CCA does not appear to be significant. This is because for this case, the large majority of the total membrane area (between 83 and 94%) and thus cost is associated with the CRM, which is unaffected by CCM permeate pressure. Similarly, in the Huang/DOE case, increasing the permeate pressures from 0.2 to 0.4 bar causes an increase of the total membrane area of about 10%, which leads to a moderate effect on the CCA. Increasing the permeate pressure to 0.6 bar causes an increase of the CCM area of almost four times with respect to the 0.4 bar pressure case and to an increase of 56% of the total membrane area. With such an increase of the membrane area, the impact of membrane cost becomes much more significant. Reducing the specific cost of the membrane improves the competitiveness of the high permeate pressure cases in terms of \$/t CO_2 avoided, because the relative contribution of the membrane to the total cost reduces while the relative contribution of the Energy Opex to the total cost increases.

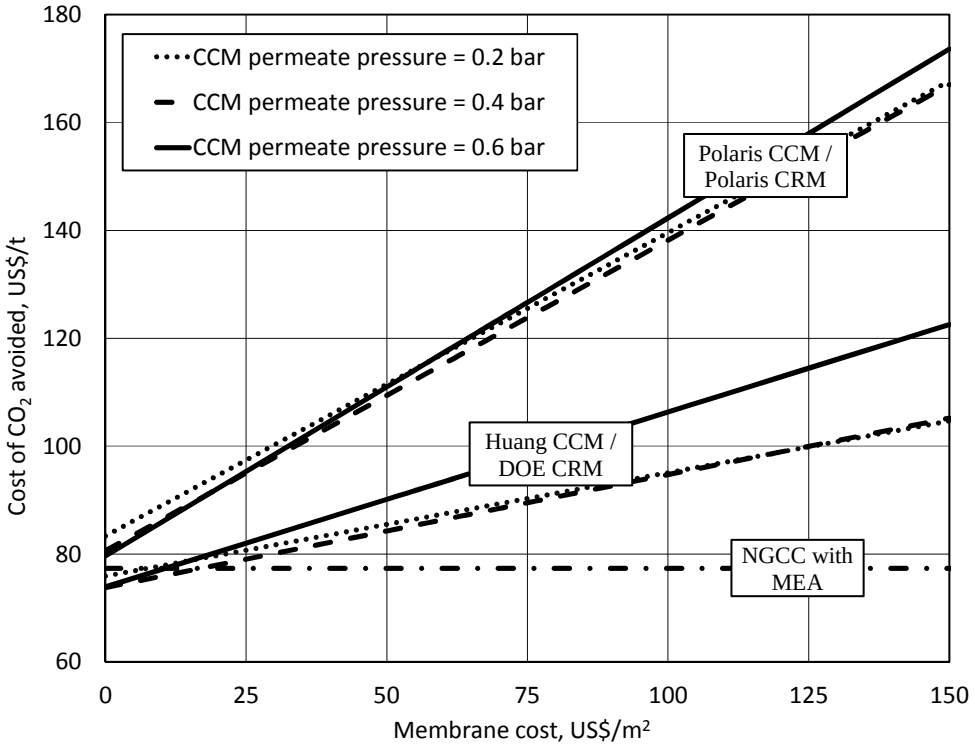

Figure 11 Cost of CO_2 avoided at different membrane costs for different membranes and CCM permeate pressures, for membrane feed pressure of 2 bar.

Figure 12 shows the effect of the specific cost of the membrane and the effect of the feed pressure for the Huang/DOE case with 0.4 bar of permeate pressure (Figure 12a) and for the Polaris/Polaris case with 0.2 bar of permeate pressure (Figure 12b). Both figures show that the specific cost of the membrane influences the choice of feed pressure significantly. In general, as the membrane cost decreases, the feed pressure that results in the lowest capture cost also decreases. This is because in this region the lower plant efficiency and the higher cost for flue gas compression and expansion are compensated by a reduction in the membrane area. For example, in the Polaris/Polaris case, at low specific membrane cost (less than about 35 $/m^2), the lowest cost of CO_2 avoided occurs at the lowest feed pressure considered of 1.5 bar. At intermediate specific membrane costs, between 35 $/m^2 and 80 $/m^2, the system with the lowest CCA is when the feed pressure is 2 bar. Once the specific membrane cost exceeds 80 $/m^2, feed pressures of 2.5 bar result in the lowest CCA. Similarly, for the Huang/DOE case for specific membrane costs below 70 $/m^2 the lowest feed pressure of 1.5 bar results in the lowest CCA, while 2 bar of feed pressure is the most competitive case for specific membrane costs above70 $/m^2. It is therefore clear that for any value of the specific membrane cost and for any combination of membranes, an optimal feed pressure exists which could be found with optimization algorithms.

For the Huang/DOE membrane system, it can be noted that at a specific membrane cost of around 45 U$/m^2 with membrane feed pressure of 1.5 bar, the system is competitive with the benchmark MEA capture case. Figure 12a reports the case with a permeate pressure of 0.4 bar. Assuming 0.2 bar as permeate pressure would produce similar trends, with a breakeven specific membrane cost with respect to the benchmark NGCC with MEA case of about 55 U$/m^2 for the feed pressure of 1.5 bar. As shown in Figure 12b for the Polaris/Polaris case, a specific membrane cost lower than 10 $/m^2 is needed to make membrane capture competitive.

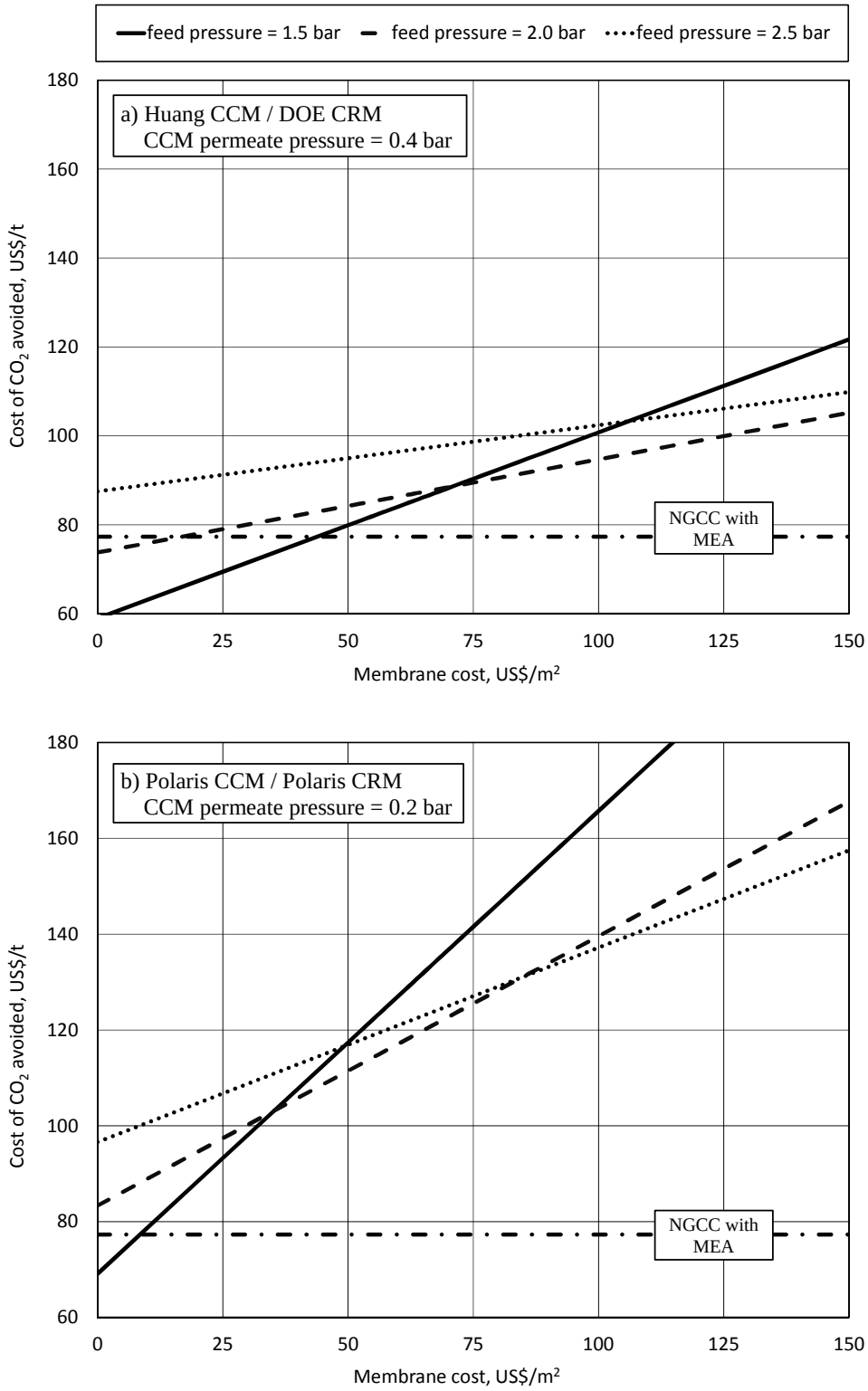

Figure 12 Cost of CO_2 avoided with variations in the specific membrane cost for different feed pressures and a reference price of

electricity (58.8 $/MWh).

In **Error! Reference source not found.**, the same analysis is performed by considering an increased electricity price of 90 $/MWh, corresponding to a scenario with a natural gas price of 12 $/GJ. In general, increasing the electricity price by 30$/MWh (i.e. comparing Figure 13**Error! Reference source not found.** with Figure 12) increases the CCA by approximately 10-15 $/t for both membrane systems when the feed pressure is 1.5 bar, and about 15 $/t when the feed pressure is about 2.5 bar. For both membrane systems, the specific membrane cost at which CCA is comparable to a NGCC with MEA capture also increases. In particular when the feed pressure is 1.5 bar, the breakeven specific membrane cost is about 65 $/m^2 for the Huang/DOE membrane case and about 18 $/m^2 for the Polaris membrane case.

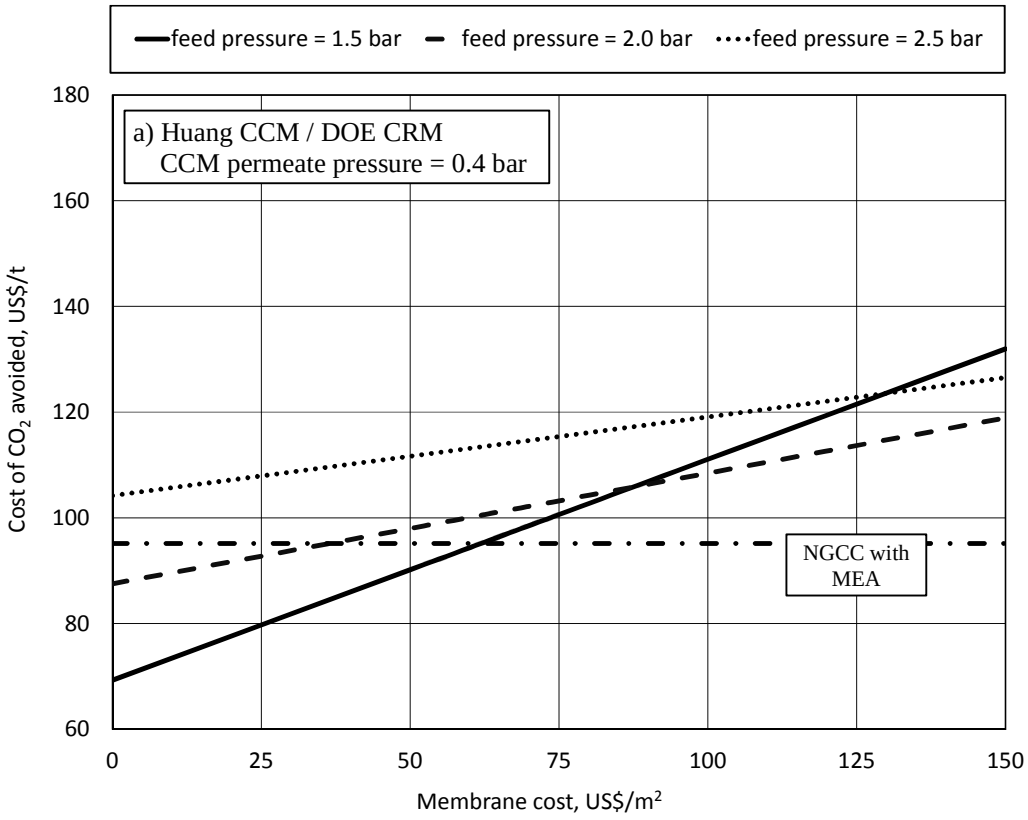

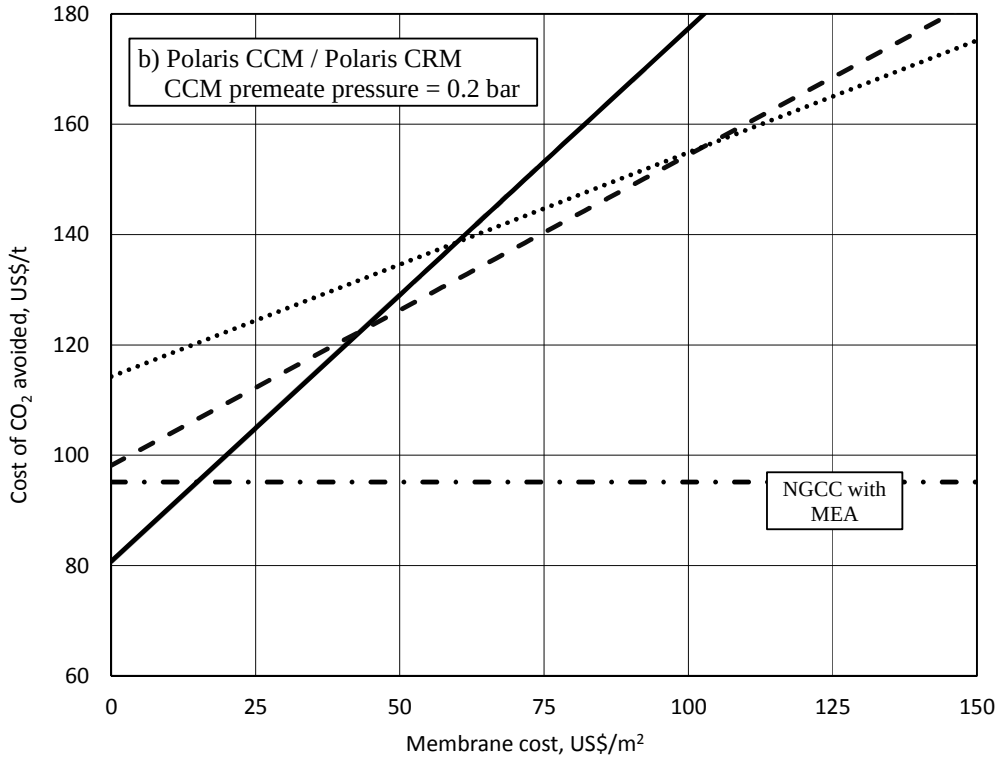

Figure 13 Cost of CO_2 avoided with variations in the specific membrane cost for different feed pressures and a price of electricity of 90 €/MWh.

Finally, the effect of the gas turbine pressure ratio is assessed. This analysis is important because of the change of the GT working fluid and its enrichment with CO_2, which has a higher molecular complexity than N_2 and O_2, which leads to a reduction of the temperature changes associated with compression and expansion with respect to a conventional GT case. For example, in the cases previously discussed with a GT pressure ratio of 18, turbine outlet temperatures (TOT) around 660°C have been obtained, which should be compared with 608°C for the reference NGCC plant. This is also reflected in the different share of the gross power output between the gas and the steam turbine, which is 60/40% in the membrane cases, vs. 65/35% in the reference NGCC (see Table 10).

Therefore, from the thermodynamic point of view, a higher pressure ratio than in the conventional case would be favourable for the cycle efficiency. On the other hand, a higher pressure ratio has a negative impact on the area of the CO_2 recycle membrane. As a matter of fact, higher pressure ratio entails higher temperature at the compressor outlet and therefore at the combustor inlet. As a consequence, higher inert gas flow rate is needed to keep the target turbine inlet temperature. Since the inert gas is provided by the selective recycle performed by the CRM, its area and cost increase when the GT pressure ratio increases.

The results of this analysis are shown in Figure 14. The region of optimal efficiency is obtained for pressure ratios between 18 and 24. It is worth noting that with a pressure ratio of 24, the TOT ranges between 603 and 612°C

depending on the membrane considered, i.e. values similar to the reference NGCC plant. This range of pressure ratio also represents the optimal range that minimizes the cost of the CO_2 avoided under the considered assumptions.

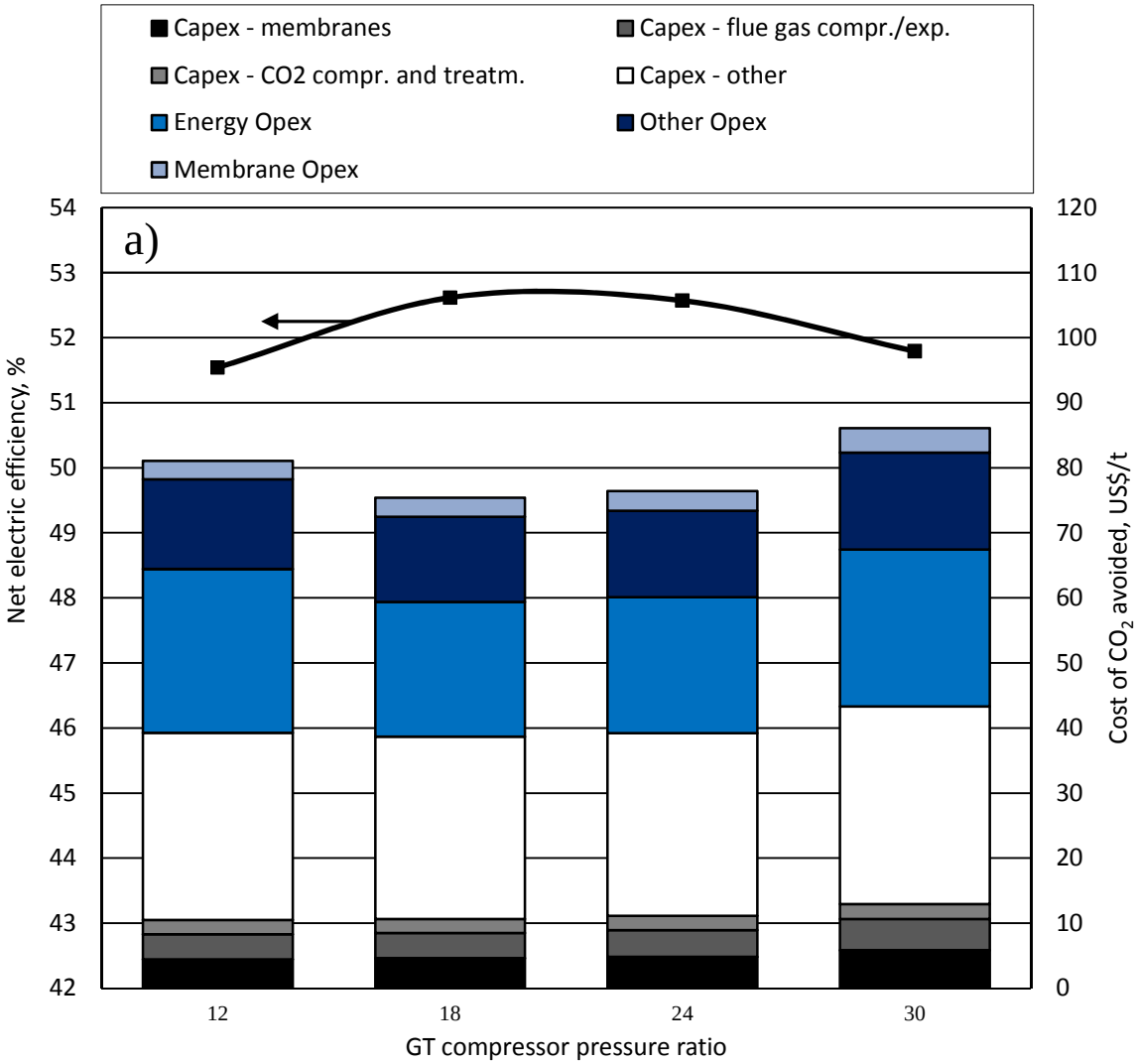

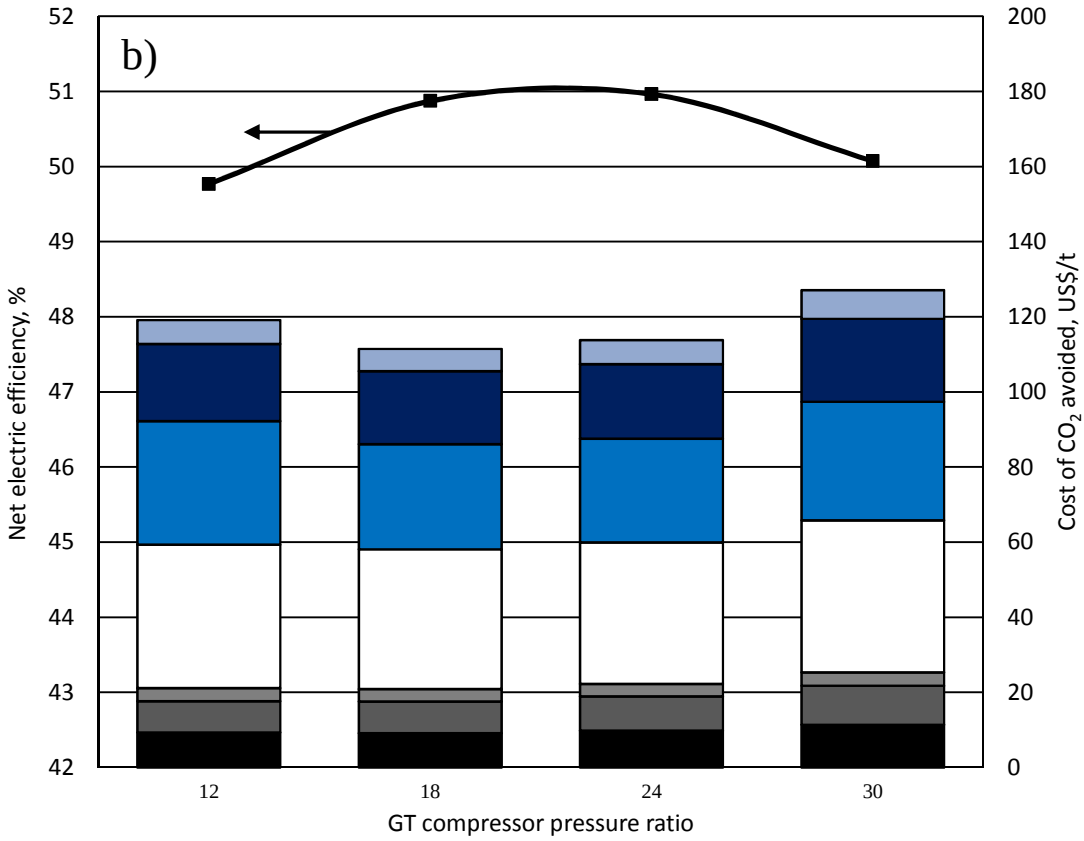

Figure 14 Cost of CO_2 avoided and plant efficiency vs. gas turbine pressure ratio for the Huang CCM / DOE CRM case with feed and CCM permeate pressures of 1.5 and 0.2 bar (a) and the Polaris/Polaris case with feed and CCM permeate pressures of 2 and 0.2 bar (b).

4 Conclusions

This paper presents a techno-economic analysis of NGCC plants with CO_2 capture using two CO_2 membranes, one for CO_2 capture and another for selective flue gas recycle. The application of three types of membranes with different permeabilities and selectivities has been assessed.

The results show that much higher efficiencies (up to about 3 percentage points) than the benchmark CO_2 capture by MEA absorption at a competitive cost of CO_2 avoided can be achieved with a target CO_2 capture rate of 90%. At a membrane cost of 50 US$/m^{2,} such performance can be obtained by combining a high selectivity and moderate permeability membrane for CO_2 capture with a high permeability and moderate selectivity membrane for the CO_2 recycle. However, to achieve significant advantages with respect to benchmark MEA capture, better membrane permeability and lower costs are needed with respect to the state of the art membranes. In addition, the need to redesign gas turbine components due to the CO_2 enriched working fluid represents a major challenge for commercial deployment of this technology.

A sensitivity analysis on the main process and economic parameters shows that a moderate pressurization of the combined cycle flue gas before feeding to the membrane system is beneficial. The optimal feed pressure largely depends on the specific cost of the membrane because it results in a trade-off between the operating costs associated with the energy consumption of the gas compressor and the membrane capital cost. The effect of gas turbine cycle pressure ratio has also been assessed due to changes in the characteristics of the gas turbine working fluid when it is enriched with CO_2. The lowest costs of CO_2 avoided and highest efficiencies are obtained with a GT pressure ratio of 18-24.

References

Allinson, G., Neal, P., Ho, M., Wiley, D., Mckee, G., 2006. CCS economics methodology and assumptions.

Aspen Technolgy, Inc., 2013. Aspen Plus Version 8.4. Burlington, MA, USA, 2013.

Brinkmann, T., Pohlmann, J., Bram, M., Zhao, L., Tota, A., Jordan Escalona, N., de Graaff, M., Stolten, D., 2015. Investigating the influence of the pressure distribution in a membrane module on the cascaded membrane system for post-combustion capture. Int. J. Greenh. Gas Control 39, 194–204. doi:10.1016/j.ijggc.2015.03.010

Bushell, A.F., Attfield, M.P., Mason, C.R., Budd, P.M., Yampolskii, Y., Starannikova, L., Rebrov, A., Bazzarelli, F., Bernardo, P., Carolus Jansen, J., Lanč, M., Friess, K., Shantarovich, V., Gustov, V., Isaeva, V., 2013. Gas permeation parameters of mixed matrix membranes based on the polymer of intrinsic microporosity PIM-1 and the zeolitic imidazolate framework ZIF-8. J. Memb. Sci. 427, 48–62. doi:10.1016/j.memsci.2012.09.035

Chiesa, P., Macchi, E., 2004. A Thermodynamic Analysis of Different Options to Break 60% Electric Efficiency in Combined Cycle Power Plants. J. Eng. Gas Turbines Power 126, 770. doi:10.1115/1.1771684

Choi, J.I., Jung, C.H., Han, S.H., Park, H.B., Lee, Y.M., 2010. Thermally rearranged (TR) poly(benzoxazole-co-pyrrolone) membranes tuned for high gas permeability and selectivity. J. Memb. Sci. 349, 358–368. doi:10.1016/j.memsci.2009.11.068

de Visser, E., Hendriks, C., Barrio, M., Mølnvik, M.J., de Koeijer, G., Liljemark, S., Le Gallo, Y., 2008. Dynamis CO_2 quality recommendations. Int. J. Greenh. Gas Control 2, 478–484. doi:10.1016/j.ijggc.2008.04.006

DOE/NETL, 2013. Cost and Performance Baseline for Fossil Energy Plants Volume 1: Bituminous Coal and Natural Gas to Electricity, NETL Report DOE/NETL-2010/1397.

DOE/NETL, 2012a. Current and Future Technologies for Power Generation with Post- Combustion Carbon Capture Final Report, NETL Report DOE/NETL-2012/1557.

DOE/NETL, 2012b. NETL Updated Costs (2011 Basis) for selected Bituminous Baseline Cases, NETL Report DOE/NETL-341/082312.

DOE/NETL, 2010. Recovery Act project: Slipstream Testing of a Membrane CO_2 Capture Process for Existing Coal-Fired Power Plants.

EBTF, 2011. European best practice guidelines for assessment of CO_2 capture technologies.

ElKady, A.M., Evulet, A., Brand, A., Ursin, T.P., Lynghjem, A., 2009. Application of Exhaust Gas Recirculation in a DLN F-Class Combustion System for Postcombustion Carbon Capture. J. Eng. Gas Turbines Power 131, 034505. doi:10.1115/1.2982158

Evulet, A.T., ELKady, A.M., Branda, A.R., Chinn, D., 2009. On the Performance and Operability of GE's Dry Low NOx Combustors utilizing Exhaust Gas Recirculation for PostCombustion Carbon Capture. Energy Procedia 1, 3809–3816. doi:10.1016/j.egypro.2009.02.182

Freeman, B.D., 1999. Basis of Permeability/Selectivity Tradeoff Relations in Polymeric Gas Separation Membranes. Macromolecules 32, 375–380. doi:10.1021/ma9814548

GECOS, 2016. GS software. www.gecos.polimi.it/software/gs.php.

González-Salazar, M.A., 2015. Recent developments in carbon dioxide capture technologies for gas turbine power generation. Int. J. Greenh. Gas Control 34, 106–116. doi:10.1016/j.ijggc.2014.12.007

Ho, M.T., Allinson, G.W., Wiley, D.E., 2008. Reducing the Cost of CO_2 Capture from Flue Gases Using Membrane Technology. Ind. Eng. Chem. Res. 47, 1562–1568. doi:10.1021/ie070541y

Huang, J., Zou, J., Ho, W.S.W., 2008. Carbon Dioxide Capture Using a CO2-Selective Facilitated Transport Membrane. Ind. Eng. Chem. Res. 1261–1267. doi:10.1021/ie070794r

Incropera, F.P., De Witt, D.P., 2002. Fundamentals of Heat and Mass Transfer, 5th ed. John Wiley & Sons.

Merkel, T.C., Lin, H., Wei, X., Baker, R., 2010. Power plant post-combustion carbon dioxide capture: An opportunity for membranes. J. Memb. Sci. 359, 126–139. doi:10.1016/j.memsci.2009.10.041

Merkel, T.C., Wei, X., He, Z., White, L.S., Wijmans, J.G., Baker, R.W., 2013. Selective exhaust gas recycle with membranes for CO2 capture from natural gas combined cycle power plants. Ind. Eng. Chem. Res. 52, 1150–1159. doi:10.1021/ie302110z

Pfaff, I., Kather, A., 2009. Comparative thermodynamic analysis and integration issues of CCS steam power plants based on oxy-combustion with cryogenic or membrane based air separation. Energy Procedia 1, 495–502. doi:10.1016/j.egypro.2009.01.066

Robeson, L.M., 2008. The upper bound revisited. J. Memb. Sci. 320, 390–400. doi:10.1016/j.memsci.2008.04.030

Scholes, C.A., Ho, M.T., Wiley, D.E., Stevens, G.W., Kentish, S.E., 2013. Cost competitive membrane—cryogenic post-combustion carbon capture. Int. J. Greenh. Gas Control 17, 341–348. doi:10.1016/j.ijggc.2013.05.017

Swisher, J.A., Bhown, A.S., 2014. Analysis and optimal design of membrane-based CO2 capture processes for coal and natural gas-derived flue gas. Energy Procedia 63, 225–234. doi:10.1016/j.egypro.2014.11.024

van Hassel, B., 2004. Oxygen transfer across composite oxygen transport membranes. Solid State Ionics 174, 253–260. doi:10.1016/j.ssi.2004.07.034

Zhao, L., Riensche, E., Blum, L., Stolten, D., 2010. Multi-stage gas separation membrane processes used in post-combustion capture: Energetic and economic analyses. J. Memb. Sci. 359, 160–172. doi:10.1016/j.memsci.2010.02.003